THE JOURNAL OF PHYSICAL CHEMISTRY B

Article

pubs.acs.org/JPCB

On the Derivation of Equilibrium Relaxation Times from Aging Experiments

Ranko Richert,*[,†] Peter Lunkenheimer,[‡] Stefan Kastner,[‡] and Alois Loidl[‡]

[†]Department of Chemistry and Biochemistry, Arizona State University, Tempe, Arizona 85287-1604, United States

[‡]Experimental Physics V, Center for Electronic Correlations and Magnetism, University of Augsburg, D-86135 Augsburg, Germany

ABSTRACT: Physical aging below the glass transition temperature, T_g, is generally understood to be governed by the same slow degrees of freedom that are responsible for structural relaxation in the equilibrium state above T_g. Provided a reliable model of aging is at hand, it should thus be possible to extract very long relaxation time constants from experimental data on physical aging. Two very different models of aging are investigated in this respect using data for various molecular glass-forming liquids extending out to aging times of 3×10^6 s. It turns out that application of the well-known KAHR or TNM model does not provide a significant advantage over a recently proposed phenomenological approach that is much simpler.

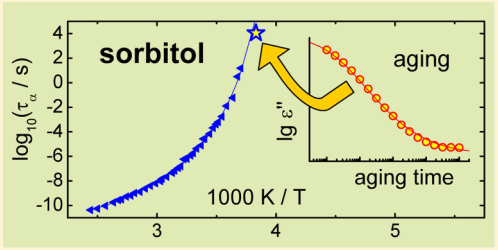

1. INTRODUCTION

Physical aging refers to the process of a glass forming liquid returning to equilibrium, usually after a temperature jump to below the glass transition temperature, T_g, where relaxation times reach values in excess of 1000 s.[1,2] The data collected in the course of physical aging is any quantity, δ, that is capable of gauging the extent of departure from equilibrium as the aging time t_{age} increases.[3] Examples for experimental observables that have been used to quantify $\delta(t_{age})$ are volume,[2] enthalpy,[4] shear modulus,[5] and dielectric loss.[6−9] The processes governing physical aging involve the same modes of structural relaxation that determine the relaxation at a constant temperature and in the regime of linear response. As a result, it should be possible to extract equilibrium relaxation time scales from an aging experiment, provided that a robust data analysis is available. If this were feasible, one could expand the range of available relaxation time data toward lower temperatures and into a regime in which relaxation time scales can be much longer than in situations where measurements of the complete correlation decay become unpractical.[10,11]

Although other protocols are possible, a typical aging measurement aims at performing a temperature jump from T_{eq} to T_{age} at a time $t = 0$ and on a time scale that is fast compared with the aging process itself. In order to follow the changes during aging in terms of $\delta(t_{age})$, the time required to determine the value of δ needs to be short compared with the time to approach equilibrium.[1] Similar to isothermal relaxation data, aging curves, $\delta(t_{age})$, can often be described by stretched exponential or Kohlrausch−Williams−Watts type decays[12,13]

$$\delta(t_{age}) = \delta_0 \exp[-(t_{age}/\tau_{age})^{\beta_{age}}] \quad (1)$$

The problem inherent in analyzing aging data is based on the fact that the relaxation time constants of the system change as the structure approaches its equilibrium state in the course of aging. This non-linear feature of the response to a temperature jump is the main obstacle in modeling aging data.[3] Several theories have been devised to address physical aging; among them are the Tool−Narayanaswamy−Moynihan (TNM)[14] and the Kovacs−Aklonis−Hutchinson−Ramos (KAHR)[15] models, both using the concept of a fictive temperature, T_f, to quantify the dependence of relaxation times τ on temperature (T) and structure (T_f).[16−19] In essence, the KAHR and TNM models are equivalent,[3,15] and they have been shown to be compatible with heterogeneous enthalpy relaxation.[20] Lunkenheimer, Wehn, Schneider, and Loidl have employed a very different approach to analyzing physical aging data,[6,21] which we will denote the LWSL model in what follows. It is simpler in the sense that it does not involve the usual non-linearity parameter, x, which partitions the dependence of τ on temperature (T) and structure (T_f) and which is often considered an adjustable parameter.[3] In this model, the change of structure is incorporated through an implicit equation for some characteristic relaxation frequency, ω_α, and its dependence on aging time[6]

$$\omega_\alpha(t_{age}) = \omega_{eq} + (\omega_{st} - \omega_{eq}) \exp[-(t_{age}/\tau_\alpha)^{\beta_{age}}], \quad \text{with}$$
$$\omega_\alpha = 1/\tau_\alpha \quad (2)$$

Because the real temperature $T = T_{age}$ is assumed constant for all times for which $\omega_\alpha(t_{age})$ is recorded, only the dependence on structure as gauged by ω_α or τ_α needs to be accounted for. Therefore, this approach does not involve a non-linearity parameter x, nor does it require the temperature dependence, $\tau_\alpha(T)$, as an input. While the above model does capture the dependence of the relaxation time constant, τ_α, on structure via

Special Issue: Peter G. Wolynes Festschrift

Received: November 11, 2012
Revised: January 3, 2013

   dx.doi.org/10.1021/jp311149n | J. Phys. Chem. B XXXX, XXX, XXX−XXX

τ_α itself, it is not equivalent to the TNM or KAHR models. In this context, it should be emphasized that the model inherent in eq 2 is meant to be a phenomenological and simple tool to extract very long relaxation times from aging data, without claiming to capture the entire physics underlying the aging mechanism.[22]

In what follows, we analyze aging results for five different molecular glass-formers on the basis of the KAHR approach and compare the results with LWSL fits following eq 2. In contrast to the model leading to eq 2, the present KAHR calculations account for the finite cooling rate of the experimental protocol and the gradual departure from equilibrium near T_g. It is demonstrated that both models generate a considerable extension of the accessible relaxation time range that reaches up to 3×10^6 s. The LWSL model, however, underestimates the values derived from extrapolating Vogel−Fulcher−Tammann (VFT)[23−25] fits to equilibrium relaxation time data, and the deviation is more pronounced for materials with higher fragility parameter m.[26−28] However, one should note that the VFT law usually does not provide perfect fits of relaxation-time data that extend over 10 decades or more, as obtained from broadband dielectric spectroscopy.[10,29−31] Therefore, a long extrapolation to large values of τ based upon the VFT relation is bound to be subject to considerable uncertainty.

2. EXPERIMENTS

The molecular glass-former D-sorbitol (purity 99%+) has been obtained from Aldrich. Precision dielectric measurements are performed at a constant sample temperature, several Kelvin below T_g, for typically 10^6 s to ensure that equilibrium was indeed reached. Parallel disk capacitors with a geometrical capacitance of around 100 pF were used. It has been estimated that the relaxation induced contraction of the sample has a negligible effect on the results. Dielectric permittivity in the frequency range 10^{-4} Hz $\leq \nu \leq 10^6$ Hz and with a resolution of $\tan\delta$ as low as 10^{-4} is measured using a Novocontrol Alpha analyzer. At selected temperatures and aging times, additional frequency sweeps at 20 Hz $\leq \nu \leq$ 1 MHz were performed with the autobalance bridges Hewlett-Packard HP4284 and HP4285.

To keep the samples at a fixed temperature for the entire aging experiment, a closed-cycle refrigerator system is used. The sample is cooled from a temperature T_g + 20 K at a cooling rate of about 3 K/min to the aging temperature T_{age} without displaying any temperature undershoot. As the zero point of the aging times reported below, we took the time when the desired temperature was reached, about 200 s after passing T_g. The temperature was kept stable within 0.02 K during the 10^6 s measurement time.

The results for propylene carbonate (PC), glycerol (GLY), xylitol (XYL), and propylene glycol (PG) were taken from the literature and were obtained using the same technique.[6,21]

3. RESULTS AND DISCUSSION

There are several factors that complicate the calculation of the process of physical aging. First, the isothermal relaxation behavior is characterized by nonexponential correlation decays,[32] and the absence of such a dispersion would simplify aging models considerably.[33] Second, the temperature dependences of the average relaxation time constants display significant departures from an Arrhenius type law. While incorporating more complex activation behavior such as the VFT law into a model of aging is straightforward, the extrapolation of fits to equilibrium data into the nonequilibrium regime below T_g is not reliable. Moreover, the description of nonequilibrium dynamics, as required in the case of aging or differential scanning calorimetry,[34] relies on modeling the dependence of the relaxation time constants on both temperature and structure. In the well-known models of aging, KAHR and TNM, the partitioning of this dependence via the non-linearity parameter x enters in a purely phenomenological fashion.[3,14,15]

Additional uncertainty regarding the most reliable approach to physical aging stems from the recognition of the heterogeneous nature of relaxation dynamics, implying that the relaxation time dispersion originates from a superposition of independent exponential modes with distinct time constants.[35−37] This well established heterogeneity of equilibrium relaxation appears to contrast the homogeneous enthalpy relaxation description of both the TNM and the KAHR models, and it suggests that a single fictive temperature is insufficient for delineating the state of the structure in a nonequilibrium situation.[38,39] Purely heterogeneous models with mode specific relaxation times and fictive temperatures have been explored,[40−42] but they do not predict the time-aging time superposition (TaTS) observed in many experiments.[6] The KAHR and TNM models both use a single variable for gauging the departure from equilibrium, thereby restoring the TaTS property,[39] but limitations of using a single fictive temperature have been pointed out by Lubchenko and Wolynes.[38] One effect of single fictive temperature models is that enthalpy relaxation is then a two-time correlation function in reduced time, implying that homogeneous and heterogeneous modeling of enthalpy relaxation become equivalent, and the apparent discrepancy between homogeneous aging models and heterogeneous equilibrium relaxation disappears.[20]

Given the uncertainties regarding models of physical aging, it appears useful to inspect the derivation of very long equilibrium relaxation times from aging data. The LWSL model uses a single variable to define the departure from equilibrium: the average relaxation time constant τ_α. As a result, the model is consistent with TaTS and with the experimental observation that the dielectric loss profile remains aging time invariant.[6]

The design of the present aging experiments and subsequent analyses does not require a temperature jump that is practically instantaneous compared with the aging process. Instead, the samples are cooled at a given constant rate and the aging time scale, t_{age}, is set to zero when the temperature has reached the targeted aging temperature, $T = T_{age}$. The first dielectric loss data is taken after 100 s, and then at a rate of 2 or 4 points per decade, i.e., equally spaced on a $\log(t_{age})$ scale. In these first 100 s, the temperature has stabilized and all changes in response to the real temperature (opposed to fictive temperature) have ceased. Therefore, the evolution of $\varepsilon''(t_{age})$ recorded in these experiments is associated only with the changes in structure. The variable used to gauge the approach of the structure toward equilibrium is usually the fictive temperature, T_f, or, equivalently, configurational temperature. Incorporating the partitioning between T and T_f via the non-linearity parameter x into a VFT type overall temperature dependence can be accomplished by the following relations[39]

$$\log_{10}\tau_0 = A + B/(T_{eff} - T_0) \quad \text{with} \quad \frac{1}{T_{eff}} = \frac{x}{T} + \frac{1-x}{T_f} \tag{3}$$

dx.doi.org/10.1021/jp311149n | J. Phys. Chem. B XXXX, XXX, XXX−XXX

which is analogous to the original TNM approach but not limited to the Arrhenius case. Clearly, x remains a relevant parameter even for the present experimental protocol, because it controls the magnitude of the apparent fictive activation energy, $\partial \log \tau_0/\partial(1/T_f)$. However, the requirement of having to use the parameters of eq 3 as an input to model calculation is circumvented in the LWSL approach by using the peak relaxation frequency, ω_α, itself as a metric for the structure and its departure from equilibrium.

In order to compare the LWSL model against the data, the implicit equation for the peak frequency of the form $\omega_\alpha = f(\omega_\alpha)$ in eq 2 is solved so that the resulting stretched exponential term describes the normalized loss versus aging time

$$\varepsilon''(t_{age}) = \varepsilon''_{eq} + (\varepsilon''_{st} - \varepsilon''_{eq}) \exp[-(t_{age}/\tau_\alpha)^{\beta_{age}}] \quad (4)$$

The stretching exponent β_{age} used in eq 2 for sorbitol is 0.30.[43] How well the approach inherent in eqs 2 and 4 describes the aging data is shown in terms of $\varepsilon''(\nu)$ versus t_{age} in Figure 1 for

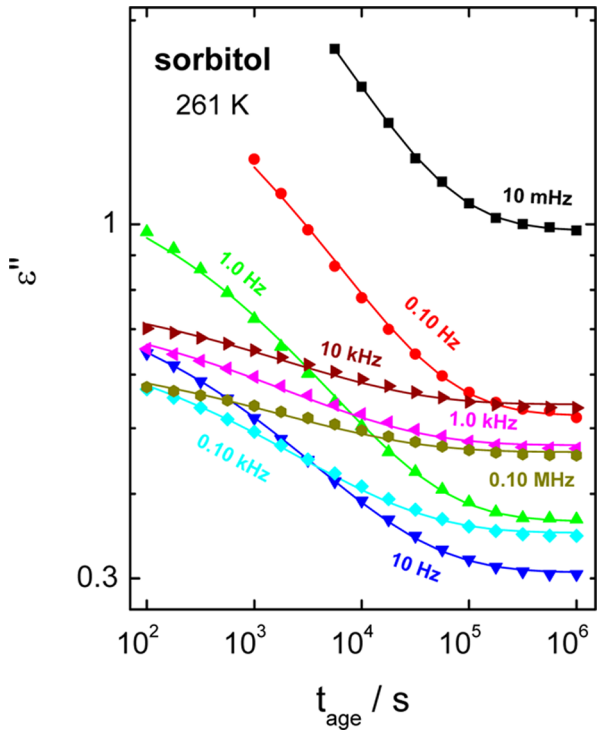

Figure 1. Symbols represent the experimental results for the dielectric loss, ε'', versus aging time, t_{age}, for sorbitol (T_{age} = 261 K) at various test frequencies between ν = 10 mHz and 100 kHz, as indicated in the legend. Lines are fits based upon the LWSL model based on a common $\nu_\alpha(t_{age})$ curve; i.e., the lines differ only in their limiting values ε''_{st} and ε''_{eq}.

various test frequencies between 10 mHz and 100 kHz. The results demonstrate that the aging dynamics are identical for all test frequencies; only the limiting values ε''_{st} and ε''_{eq} are frequency specific (and consistent with equilibrium data).[6] As has been found for analogous measurements of other compounds,[6,21] TaTS applies across a large range of test frequencies for the present experimental conditions. Even for sorbitol with its considerable secondary relaxation amplitude and very high fragility (m = 117), the solid lines that reflect the LWSL model provide very good fits to these aging data.

Upon the basis of a test frequency of ν = 1 Hz for all cases, Figure 2 emphasizes that the LWSL approach captures the

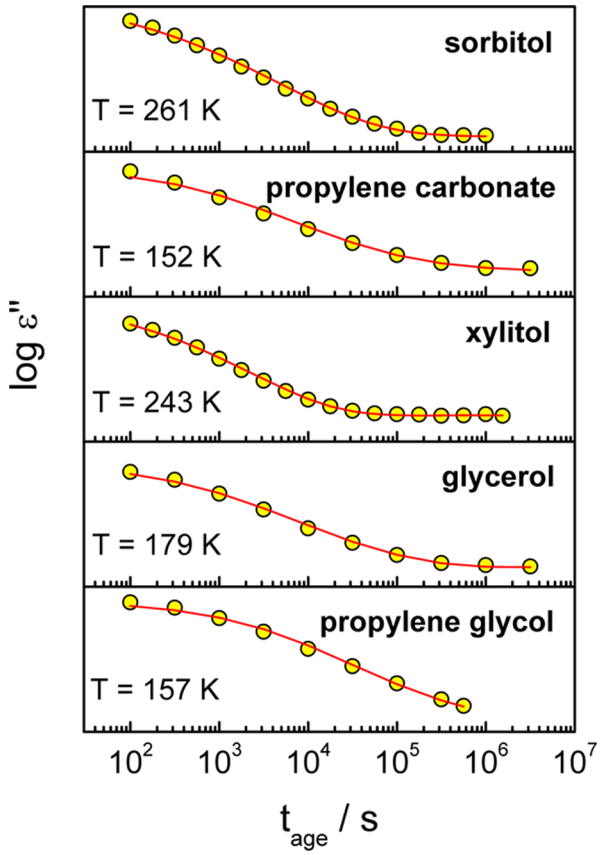

Figure 2. Symbols represent the experimental results for the dielectric loss, ε'', at the frequency ν = 1 Hz as a function of aging time, t_{age}, for D-sorbitol (SOR) and four other glass-formers PC, XYL, GLY, and PG at the aging temperatures indicated. Lines are fits based upon the LWSL model. The ordinates are logarithmically scaled using the following ranges in terms of ε'': SOR, 0.32−1.1; PC, 0.03−0.3; XYL, 0.3−1; GLY, 0.08−0.4; PG, 0.027−0.1.

aging dynamics for a series of glass forming liquids that differ considerably in their fragility m. The fits shown as solid lines are based on the stretching exponents, β_{age}, listed in Table 1. The main parameter of current interest that can be extracted from such fits is the equilibrium peak relaxation time at the aging temperature, $\tau_{LWSL} = \tau_\alpha(T_{age})$. The question that remains is how accurately will such $\tau_\alpha(T_{age})$ values reflect what would be obtained from a true equilibrium relaxation time experiment at $T = T_{age}$. First, the LWSL approach is not derived from a rigorous model of aging. Second, at first glance, the application of eqs 2 and 4 to loss data, $\varepsilon''(\nu)$, is straightforward only for systems with a Debye type loss peak, where the high frequency wing is characterized by a slope of $d\lg\varepsilon''/d\lg\nu = -1$. The origin of this assumption is the linear relation between $\varepsilon''(t_{age})$ and $\omega_\alpha(t_{age})$ which emerges from eliminating the exponential term in eq 4 by inserting that of eq 2, which yields

$$\frac{\varepsilon''(t_{age}) - \varepsilon''_{eq}}{\varepsilon''_{st} - \varepsilon''_{eq}} = \frac{\omega_\alpha(t_{age}) - \omega_{eq}}{\omega_{st} - \omega_{eq}} \quad (5)$$

For liquids displaying a relaxation time dispersion, eq 5 will remain an approximation. For such liquids, the high frequency ($\omega \gg \omega_\alpha$) slope $d\lg\varepsilon''/d\lg\omega = -s$ with $s < 1$ yields a non-linear

dx.doi.org/10.1021/jp311149n | J. Phys. Chem. B XXXX, XXX, XXX−XXX

Table 1. Relaxation and Aging Characteristics for the Five Glass-Formers of This Study[a]

	T_g (K)	m	β_{age}	T_{age} (K)	$\log_{10}(\tau_{LWSL}$ (s))	$\log_{10}(\tau_{KAHR}$ (s))	$\Delta\log_{10}(\tau)$
SOR	274	117	0.30	261	4.04	5.30	1.26
PC	159	112	0.60	152	5.52	6.51	0.99
XYL	248	94	0.43	243	3.56	3.42	−0.14
GLY	185	53	0.55	179	4.81	5.08	0.27
PG	167	52	0.58	157	5.80	6.28	0.48

[a]Glass transition temperature T_g, fragility index m, stretching exponent of the LWSL model β_{age}, aging temperature T_{age}, logarithmic relaxation times τ_{LWSL} and τ_{KAHR} at $T = T_{age}$ associated with the LWSL and KAHR models, respectively. The values of $\Delta\log_{10}(\tau)$ are defined as $\log_{10}(\tau_{KAHR}/\tau_{LWSL})$.

dependence of ε'' on ω_α, while eq 5 implies proportionality if TaTS is assumed.[44] Therefore, the application of this model to cases with non-Debye type high frequency slopes, $d\lg\varepsilon''/d\lg\omega > -1$, warrants further inspection.

As an alternative to the above analysis of the aging data, we test to what extent the experimental results are consistent with the KAHR type model of physical aging. As the single fictive temperature version is adopted here, this KAHR model is compatible with dynamic heterogeneity (and homogeneity) regarding the enthalpy relaxation.[20] The fictive temperature is calculated via the standard expression[3,14]

$$T_f(T) = T_{eq} + \int_{T_0}^{T}\left(1 - \exp\left(-\left(\int_{T'}^{T}\frac{dt''}{\tau_0}\right)^{\beta}\right)\right)dT' \quad (6)$$

with the initial (equilibrium state) temperature T_{eq} set to T_g + 20 K as in the experiment. To mimic the experimental protocol, the real temperature T is assumed to approach T_{age} at a rate of −3 K/min and then kept constant at T_{age}. The characteristic time constant is determined according to eq 3. This requires the VFT parameters A, B, and T_0, the non-linearity parameter x, as well as the stretching exponent β as input. The impact of the peak frequency $\omega_\alpha = 1/\tau_\alpha$ on the dielectric loss, ε'', is based upon a power law behavior for the high frequency wing, $d\lg\varepsilon''/d\lg\omega_\alpha = s$, and the values used for s were guided by the slopes observed above T_g. The parameters entering the calculation for the five compounds are compiled in Table 2, with the VFT

Table 2. Parameters Entering the KAHR Model Calculation[a]

	T_{age} (K)	A	B (K)	T_0 (K)	β	x	s
SOR	261	−13.46	543.9	232	0.45	0.32	0.68
PC	152	−12.61	299.5	136.5	0.60	0.30	0.54
XYL	243	−13.79	653.8	205	0.48	0.48	0.40
GLY	179	−14.81	994.3	129	0.55	0.41	0.58
PG	157	−13.79	805.6	117	0.62	0.50	0.55

[a]Aging temperature T_{age}, VFT constants A, B, and T_0, stretching exponent β, non-linearity parameter x, slope $s = d\lg\varepsilon''/d\lg\omega_\alpha$.

constants determined from equilibrium dielectric relaxation data. These KAHR model calculations are shown as solid lines in Figure 3 and compared with the same data sets displayed already in Figure 2. By comparing these two figures, it is obvious that both the LWSL and the KAHR model provide descriptions of the data of comparable quality. Because the KAHR model accounts for the entire cooling process beginning at T_g + 20 K, the non-linearity parameter x is relevant for partitioning the dependence of τ_α on temperature (T) and on structure (T_f) using eq 3. Consistent with previous results regarding the non-linearity,[3,38] the value of x tends to be smaller for the more fragile materials. With considerable margin of error, the correlation can be expressed as $m = 33/x$ obtained

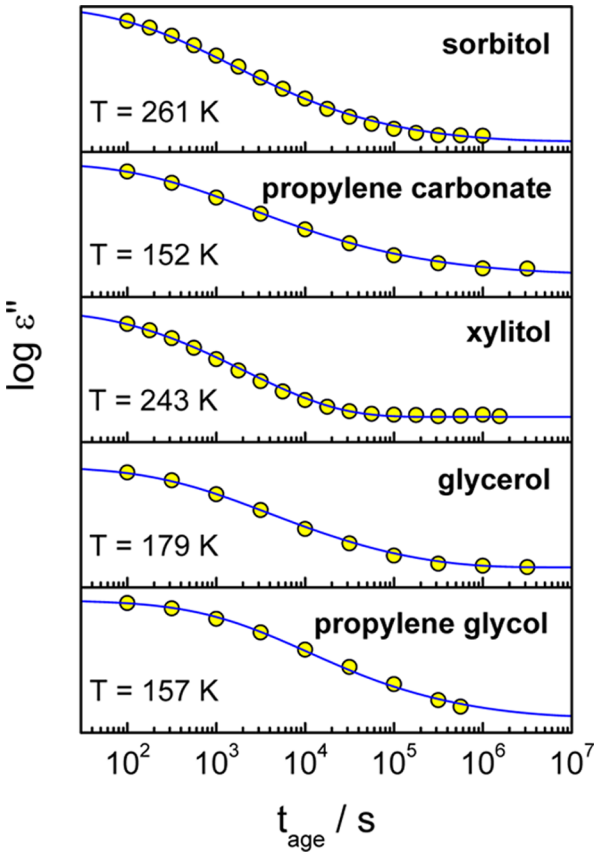

Figure 3. Symbols represent the experimental results for the dielectric loss, ε'', at the frequency ν = 1 Hz as a function of aging time, t_{age}, for D-sorbitol (SOR) and four other glass-formers PC, XYL, GLY, and PG at the aging temperatures indicated. Lines are calculations based upon the KAHR model using the parameters listed in Table 2. See Figure 1 for the ordinate scaling.

from a hyperbolic fit, analogous to the $m = m_{min}/x$ relation reported by Böhmer,[45] and to the $m = 19/x$ result stated by Lubchenko and Wolynes.[38] In contrast to the LWSL case where $\tau_{LWSL} = \tau_\alpha(T_{age})$ is an output of the fit process, the relaxation time $\tau_{KAHR} = \tau_\alpha(T_{age})$ is an input to the KAHR model via the extrapolation of the VFT relation that describes $\tau_\alpha(T)$ in the equilibrium range, $T > T_g$. The values for τ_{KAHR} as well as the logarithmic differences $\Delta\log_{10}(\tau) = \log_{10}(\tau_{KAHR}/\tau_{LWSL})$ are included in Table 1.

The activation behavior of the five compounds of this study is depicted in Figure 4. The stars represent the τ_α values as extrapolated via the VFT relation to $T = T_{age}$; i.e., they are the end points at T_{age} and τ_{KAHR} of the VFT curves shown as solid lines. The open diamonds indicate the values of τ_{LWSL} as derived from fits to $\varepsilon''(t_{age})$ using the LWSL expressions, eqs 2 and 4. One can observe that τ_{LWSL} is smaller than τ_{KAHR}, and

dx.doi.org/10.1021/jp311149n | J. Phys. Chem. B XXXX, XXX, XXX−XXX

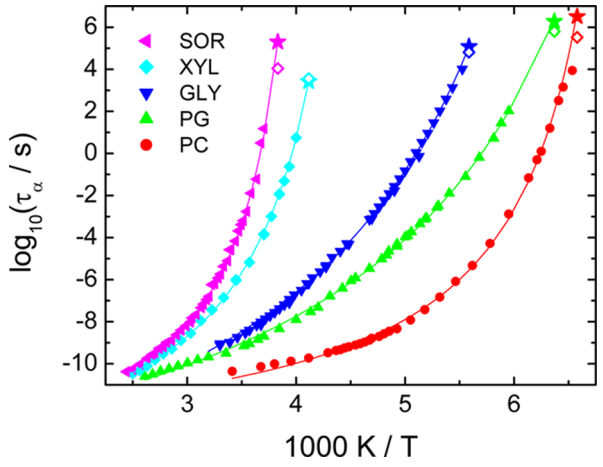

Figure 4. Solid symbols represent the experimental results for the equilibrium dielectric relaxation times, τ_α, as a function of temperature for D-sorbitol (SOR) and four other glass-formers PC, XYL, GLY, and PG. Lines are VFT fits using the parameters listed in Table 2. Open diamonds represent the values of $\tau_\alpha(T_{age})$ obtained from the LWSL analysis of aging data, and stars identify the relaxation times τ_α of the VFT fits if extrapolated to $T = T_{age}$.

that the discrepancy tends to increase with increasing fragility index m (see also Table 1, $\Delta\log_{10}(\tau)$ versus m). A plausible reason for this difference, $\Delta\log_{10}(\tau)$, generally being positive can be seen in Figure 5, a graph of the normalized quantities

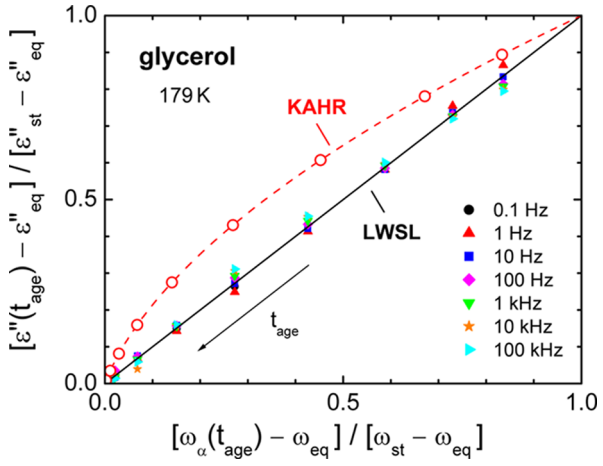

Figure 5. Normalized quantities, ε'' versus ν_α, for glycerol at T_{age} = 179 K. Symbols along the identity line are experimental $\varepsilon''(t_{age})$ results associated with $\nu_\alpha(t_{age})$ values derived from the LWSL analysis. Data are for various test frequencies, as indicated. The dashed line reflects the ε'' versus ν_α dependence derived from the KAHR calculation, with the open symbols matching the aging times of the experiment.

$\varepsilon''(t_{age})$ versus $\omega_\alpha(t_{age})$. According to eq 5, the LWSL approach implies the identity relation in this plot and, accordingly, the $\omega_\alpha(t_{age})$ values derived from this model obey the expected relation for all test frequencies. By contrast, the ε'' and ω_α values extracted from the KAHR calculation for the same set of aging times follow a different path, and the discrepancy is largely governed by the slope parameter s. At very long aging times (lower left corner in Figure 5), a certain change in ε'' translates into a larger change of ω_α per unit time and thus into a lower relaxation time constant in the LWSL analysis compared with the KAHR case.

Because of the uncertainties of the parameters x and s entering the KAHR calculation, the necessity to extrapolate the temperature dependence, and the assumption of TaTS, the present KAHR model results do not go beyond demonstrating the possible consistency between a more rigorous model of physical aging and experimental aging data. Therefore, the extrapolations of the VFT fits to τ_{KAHR} at T_{age} are in no way more reliable than the τ_{LWSL} counterparts. For example, if the Vogel temperature T_0 of sorbitol is decreased by 2 K, the resulting VFT curve matches τ_{LWSL} at T_{age}, while remaining consistent with the higher temperature dielectric relaxation data. Adjusting the non-linearity to $x = 0.49$ when T_0 is set to 230 K yields a description of the aging data that is at least as good as the one shown in Figure 3 for $T_0 = 232$ K and $x = 0.32$. As the value of x cannot be obtained from an independent source, the relaxation time constant τ_{LWSL} is also compatible with the aging data if judged on the basis of the KAHR model of physical aging.

4. SUMMARY AND CONCLUSIONS

For five molecular glass-forming liquids that differ considerably in their fragility index m, aging isotherms recorded out to 3×10^6 s can be described well by two conceptually different approaches to physical aging. The KAHR (or equivalently the TNM) model is more general in terms of its ablity to handle complex temperature protocols as in the case of a DSC experiment, whereas the LWSL approach is limited to aging isotherms. Because only the variation of structure is relevant at a constant aging temperature, aging isotherms are the results of choice for obtaining very large relaxation time constants. While the KAHR model provides a more rigorous physical picture for understanding the aging dynamics, uncertainties in the non-linearity parameter x and in the net number of fictive temperatures prohibit its use as a straightforward tool for deriving $\tau_\alpha(T_{age})$ from aging isotherms.

The LWSL model arrives at the relaxation time constant $\tau_\alpha(T_{age})$ mainly by capturing the rate of approach to equilibrium while assuming that deviations from TaTS are negligible. The latter ensures that changes in the dielectric loss at relatively high frequencies properly reflect the shift of the most probable or average relaxation time. By virtue of eq 5, the model rests on an approximation that is more justifiable for supercooled liquids that do not display high values of the fragility index m. Accordingly, Figure 5 suggests that reliable relaxation time constants of up to 10^6 s can be derived from aging isotherms for cases with a fragility of $m < 100$, while higher and systematic errors are expected for $m > 100$ systems.

In conclusion, aging isotherms can be used to expand the experimental range of relaxation time data, but our understanding of aging has not yet reached a level of microscopic understanding where predictions far from equilibrium become possible. Significant advances would emerge from a physical basis for the non-linearity parameter x and from understanding the existence or lack of spatial and spectral distribution of fictive temperatures. Only few studies emphasize the significance of these aspects.[20,38,39]

AUTHOR INFORMATION

Corresponding Author

*E-mail: ranko@asu.edu.

Notes

The authors declare no competing financial interest.

dx.doi.org/10.1021/jp311149n | J. Phys. Chem. B XXXX, XXX, XXX−XXX

■ ACKNOWLEDGMENTS

Help with numerical calculations from S. K. S. Mazinani is gratefully acknowledged. We thank L. C. Pardo for performing the aging measurements of sorbitol. This material is based upon work supported by the National Science Foundation under Grant No. CHE-1026124 (International Collaboration in Chemistry). The work at the University of Augsburg was supported by the Deutsche Forschungsgemeinschaft via Research Unit FOR1394.

■ REFERENCES

(1) *Physical aging in amorphous polymers and other materials*; Struick, L. C. E., Ed.; Elsevier: Amsterdam, The Netherlands, 1978.
(2) Kovacs, A. J. *J. Polym. Sci.* **1958**, *30*, 131−147.
(3) Hodge, I. M. *J. Non-Cryst. Solids* **1994**, *169*, 211−266.
(4) Takeda, K.; Yamamuro, O.; Suga, H. *J. Phys. Chem.* **1995**, *99*, 1602−1607.
(5) Shi, X.; Mandanici, A.; McKenna, G. B. *J. Chem. Phys.* **2005**, *123*, 174507.
(6) Lunkenheimer, P.; Wehn, R.; Schneider, U.; Loidl, A. *Phys. Rev. Lett.* **2005**, *95*, 055702.
(7) Hecksher, T.; Olsen, N. B.; Niss, K.; Dyre, J. C. *J. Chem. Phys.* **2010**, *133*, 174514.
(8) Preuß, M.; Gainaru, C.; Hecksher, T.; Bauer, S.; Dyre, J. C.; Richert, R.; Böhmer, R. *J. Chem. Phys.* **2012**, *137*, 144502.
(9) Leheny, R. L.; Nagel, S. R. *Phys. Rev. B* **1998**, *57*, 5154−5162.
(10) Lunkenheimer, P.; Kastner, S.; Köhler, M.; Loidl, A. *Phys. Rev. E* **2010**, *81*, 051504.
(11) Pimenov, A.; Loidl, A.; Böhmer, R. *J. Non-Cryst. Solids* **1997**, *212*, 89−94.
(12) Kohlrausch, R. *Pogg. Ann. Phys. Chem.* **1854**, *91*, 179−214.
(13) Williams, G.; Watts, D. C. *Trans. Faraday Soc.* **1970**, *66*, 80−85.
(14) Moynihan, C. T.; Macedo, P. B.; Montrose, C. J.; Gupta, P. K.; DeBolt, M. A.; Dill, J. F.; Dom, B. E.; Drake, P. W.; Easteal, A. J.; Elterman, P. B.; et al. *Ann. N.Y. Acad. Sci.* **1976**, *279*, 15−35.
(15) Kovacs, A. J.; Aklonis, J. J.; Hutchinson, J. M.; Ramos, A. R. *J. Polym. Sci., Polym. Phys. Ed.* **1979**, *17*, 1097−1162.
(16) Tool, A. Q.; Eichlin, C. G. *J. Am. Ceram. Soc.* **1931**, *14*, 276−308.
(17) Tool, A. Q. *J. Am. Ceram. Soc.* **1946**, *29*, 240−253.
(18) Gardon, R.; Narayanaswamy, O. S. *J. Am. Ceram. Soc.* **1970**, *53*, 380−385.
(19) Narayanaswamy, O. S. *J. Am. Ceram. Soc.* **1971**, *54*, 491−498.
(20) Mazinani, S. K. S.; Richert, R. *J. Chem. Phys.* **2012**, *136*, 174515.
(21) Lunkenheimer, P.; Wehn, R.; Loidl, A. *J. Non-Cryst. Solids* **2006**, *352*, 4941−4945.
(22) An alternative to eq 2 was proposed in: Gupta, S.; Das, S. P. *Phys. Rev. E* **2007**, *76*, 061502.
(23) Vogel, H. *Phys. Z.* **1921**, *22*, 645−646.
(24) Fulcher, G. S. *J. Am. Ceram. Soc.* **1925**, *8*, 339−355.
(25) Tammann, G.; Hesse, W. *Z. Anorg. Allg. Chem.* **1926**, *156*, 245−257.
(26) Angell, C. A. *J. Non-Cryst. Solids* **1991**, *131−133*, 13−31.
(27) Böhmer, R.; Angell, C. A. *Phys. Rev. B* **1992**, *45*, 10091−10094.
(28) Böhmer, R.; Ngai, K. L.; Angell, C. A.; Plazek, D. J. *J. Chem. Phys.* **1993**, *99*, 4201−4209.
(29) Schönhals, A.; Kremer, F.; Hofmann, A.; Fischer, E. W.; Schlosser, E. *Phys. Rev. Lett.* **1993**, *70*, 3459−3462.
(30) Stickel, F.; Fischer, E. W.; Richert, R. *J. Chem. Phys.* **1995**, *102*, 6251−6257.
(31) Stickel, F.; Fischer, E. W.; Richert, R. *J. Chem. Phys.* **1996**, *104*, 2043−2055.
(32) Angell, C. A.; Ngai, K. L.; McKenna, G. B.; McMillan, P. F.; Martin, S. W. *J. Appl. Phys.* **2000**, *88*, 3113−3157.
(33) Chen, K.; Schweizer, K. S. *Phys. Rev. E* **2008**, *78*, 031802.
(34) Weyer, S.; Merzlyakov, M.; Schick, C. *Thermochim. Acta* **2001**, *377*, 85−96.
(35) Ediger, M. D. *Annu. Rev. Phys. Chem.* **2000**, *51*, 99−128.
(36) Richert, R. *J. Phys.: Condens. Matter* **2002**, *14*, R703−R738.
(37) Richert, R.; Israeloff, N.; Alba-Simionesco, C.; Ladieu, F.; L'Hôte, D. In *Dynamical Heterogeneities in Glasses, Colloids, and Granular Media*; Berthier, L., Biroli, G., Bouchaud, J.-P., Cipelletti, L., van Saarloos, W., Eds.; Oxford University Press: Oxford, U.K., 2011; pp 152−202.
(38) Lubchenko, V.; Wolynes, P. G. *J. Chem. Phys.* **2004**, *121*, 2852−2865.
(39) Richert, R. *J. Chem. Phys.* **2011**, *134*, 144501.
(40) Saika-Voivod, I.; Sciortino, F. *Phys. Rev. E* **2004**, *70*, 041202.
(41) Diezemann, G. *J. Chem. Phys.* **2005**, *123*, 204510.
(42) Richert, R. *Phys. Rev. Lett.* **2010**, *104*, 085702.
(43) This value was determined from a fit of the equilibrium spectrum at 261 K and has a high uncertainty due to a relatively strong conductivity contribution found in sorbitol at low temperatures. See: Kastner, S.; Köhler, M.; Goncharov, Y.; Lunkenheimer, P.; Loidl, A. *J. Non-Cryst. Solids* **2011**, *357*, 510−514. However, we have checked that using a value of 0.5 (also compatible with the equilibrium results) leads to a reasonable description of the aging data, too, resulting in a similar equilibrium relaxation time of 1.8×10^4 s instead of 1.1×10^4 s.
(44) However, it should be noted that eq 5 corresponds to $\varepsilon'' = a + b\omega_\alpha$ (with a and b representing constants) and the nonzero offset a leads to $d\lg\varepsilon''/d\lg\omega_\alpha \neq 1$, at least for small ω_α.
(45) Böhmer, R. *J. Non-Cryst. Solids* **1994**, *172−174*, 628−634.